This is a preprint of a paper intended for publication in a journal or proceedings. Since changes may be made before publication, this preprint is made available with the understanding that it will not be cited or reproduced without the permission of the author.

UCRL - 74797
PREPRINT
Conf-731112--12

LAWRENCE LIVERMORE LABORATORY
University of California/Livermore, California

DUAL ENERGY ANALYSIS USING PHOSWICH SCINTILLATION DETECTORS FOR LOW-LEVEL IN-VIVO COUNTING

E.G. Shapiro
A.L. Anderson

October 3, 1973

NOTICE
This report was prepared as an account of work sponsored by the United States Government. Neither the United States nor the United States Atomic Energy Commission, nor any of their employees, nor any of their contractors, subcontractors, or their employees, makes any warranty, express or implied, or assumes any legal liability or responsibility for the accuracy, completeness or usefulness of any information, apparatus, product or process disclosed, or represents that its use would not infringe privately owned rights.

This paper was prepared for the IEEE Nuclear Science Symposium, November 14-16, 1973, San Francisco, and for subsequent publication in IEEE Transactions on Nuclear Science.

MASTER

DISTRIBUTION OF THIS DOCUMENT IS UNLIMITED

DUAL ENERGY ANALYSIS USING PHOSWICH SCINTILLATION DETECTORS FOR LOW-LEVEL IN-VIVO COUNTING*

E.G. Shapiro and A.L. Anderson

University of California, Lawrence Livermore Laboratory
Livermore, California 94550

Summary

Electronics developed for a whole body counting system analyze the pulse heights of signals from both the sodium iodide (NaI(Tl)) and cesium iodide (CsI(Na)) crystals of a phoswich scintillation detector. Pulse shape discrimination is used to determine the origin of the scintillation, NaI or CsI, while rejecting coincident Compton-scattered events and photomultiplier tube noise. Both energy spectra are accumulated simultaneously in separate memory quadrants of a multichannel analyzer. The system allows for low-energy (5 keV - 125 keV) x-ray analysis from the NaI(Tl) crystal and high-energy (100 keV - 2.5 MeV) x-ray or γ-ray analysis from the CsI(Na) crystal. The discrimination system is better than 95% efficient over both energy ranges, with a low-energy (12-24keV) shielded background count of less than 2 cpm for a single 5-in.-diam phoswich detector. This system thus extends the detector's normal energy range by more than an order of magnitude.

Introduction

Many authors have utilized phoswich/twin-crystal detectors for low-level x-ray detection.[1-5] Briefly, a phoswich x-ray scintillation detector consists of a thin NaI(Tl) crystal coupled optically to a single photomultiplier tube. The NaI crystal is used to detect low-energy (less than 125 keV) photons, while the CsI crystal acts as an anticoincidence shield for higher-energy Compton-scattered events. Pulse shape discrimination (PSD) is then used to accept events with the characteristic 0.25 μs fluorescence decay time of the NaI(Tl) crystal and reject events with the 1.1 μs fluorescence decay time of the CsI(Na) crystal or any composite decay time of the two scintillators, i.e., coincident Compton events. A block diagram of such a detection system appears in Fig. 1. This configuration typically yields shielded background counting rates as low as 2 cpm for a 5-in. detector over a 12-24 keV energy region with a 95% relative counting efficiency for the 17 and 60 keV x-rays of ^{241}Am. It should be noted that 100% efficiency is the efficiency of the detector without PSD. This system is used widely for low-level whole body in-vivo lung counting for plutonium, and it was the configuration used previously in the LLL Whole Body Counter. The additional capability of analyzing the higher-energy (0.1 - 2.5 MeV) γ-ray events detected by the CsI(Na) crystal along with the low-energy NaI(Tl) x-ray event has been achieved. This additional information is directly useful

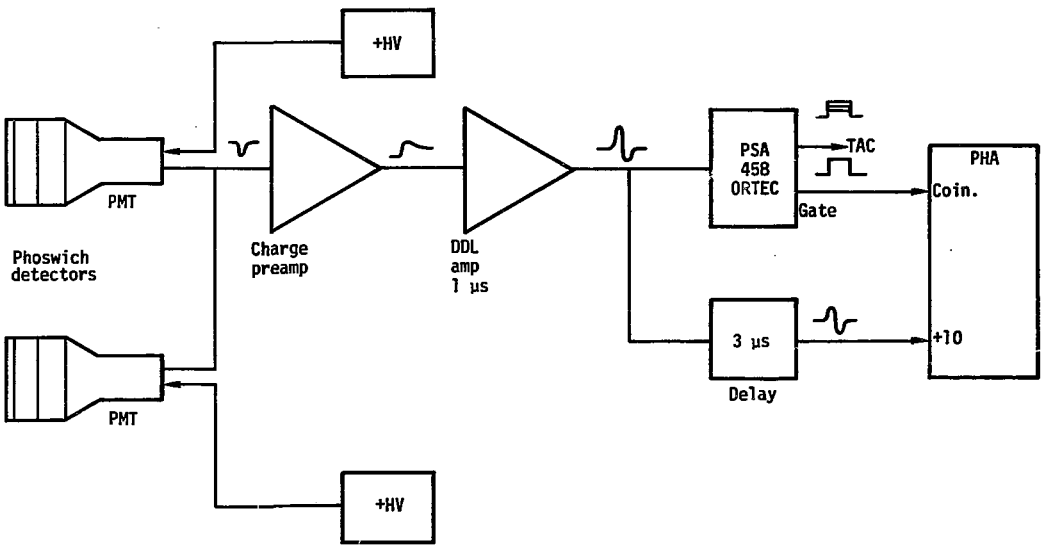

Fig. 1. Diagram of the phoswich low-energy detection system.

*This work performed under the auspices of the U.S. Atomic Energy Commission.

in accessing any high-energy emitters within the body. Also, the higher-energy spectrum can be useful in obtaining correlation between a human's high-level and low-level background spectra.[6] This would provide a more accurate means of accessing ones natural, uncontaminated low-level background when assaying for plutonium or other low-energy photon emitters. A detailed description of this dual energy analysis system will be presented, and it will be compared with a single crystal detector system.

Detector Characteristics

Before describing the electronics used to obtain the dual energy spectrum, a brief description of the phoswich detector and its scintillation time spectrum is required. The detector construction appears in Fig. 2. Figure 3 shows the possible photon interactions that can occur within the crystals.[4] The photoelectric conversions are the events to be accepted, and the Compton interactions in both crystals are the events to be rejected. Figure 4 displays the curves for the percentage of interactions vs photon energy for the phoswich detector. The curves were generated using the published[7] photon cross-section data for NaI and CsI. The percentage of photoelectric interaction in each crystal illustrates the detector's collection efficiency.

Figure 5 shows a typical scintillator decay-time spectrum from two phoswich detectors with a ^{137}Cs source. The smaller time peak is a result of the lower-energy 32-keV x-rays detected solely by the NaI crystal yielding its characteristic 0.25-μs fluorescence decay. The larger time peak is generated by the more-abundant, higher-energy (662 keV) ^{137}Cs γ-rays that pass through the thin NaI crystal and are detected by the thicker CsI crystal, which yields its characteristic 1.1 μs fluorescence decay signal. The valley between the peaks represents the Compton-scattered events that have composite time spectra dependent upon the amount of recoil electron energy deposited in each crystal. Figure 6 shows a typical decay time spectrum in a shielded air background from two phoswich detectors. As before, both the NaI and CsI peaks appear, but the Compton-scattered events are masked by cosmic ray overloads that saturate the electronics. Therefore, a cosmic ray overload blanking circuit was incorporated to prevent spurious signals from being counted. This resulted in a 40% reduction in the 12-24 keV background. Just to the left of the NaI peak is the faster photomultiplier tube (PMT) noise region, which is a result of thermionic electrons generated at the PMT photocathode and dynodes.

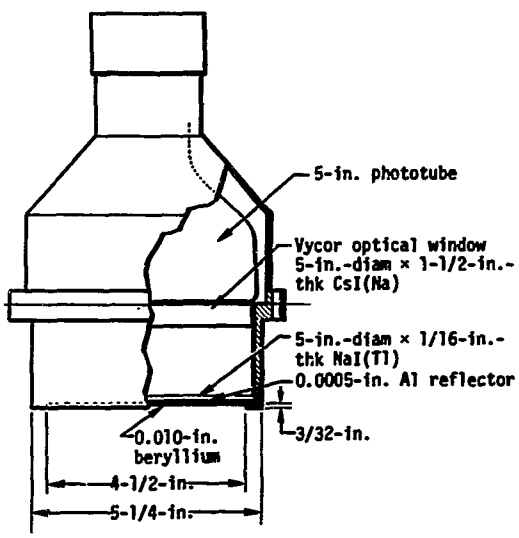

Fig. 2. Phoswich detector construction.

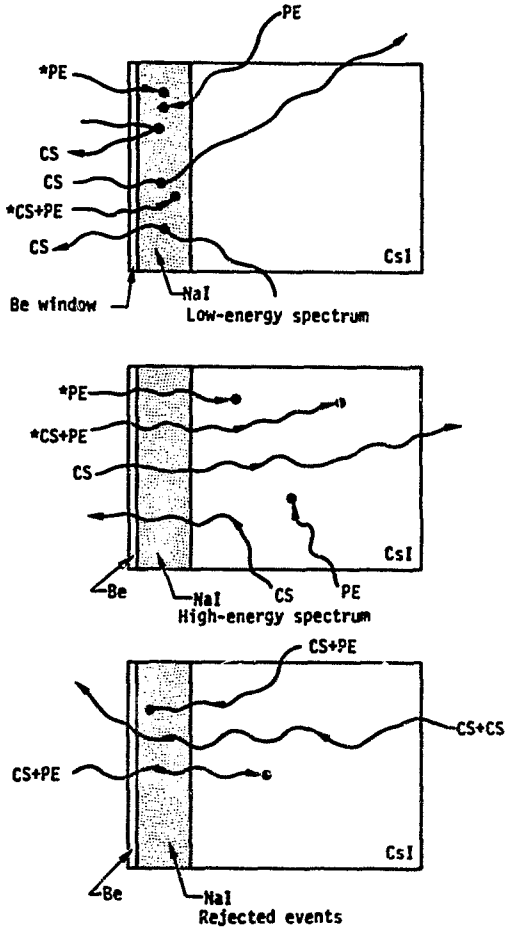

Fig. 3. Possible photon interactions with phoswich crystals. Photoelectric (PE) and Compton Scatter (CS) without pair production. Asterisk indicates desirable.

Low-Energy Analysis

When low-level photons are detected, the NaI events are selected on the basis of scin-

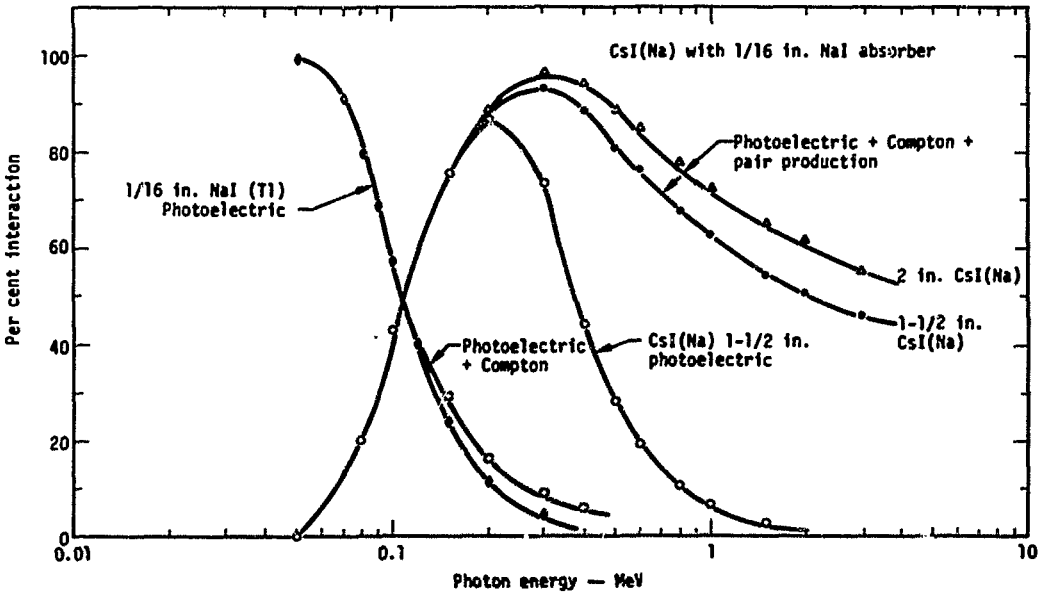

Fig. 4. Percentage of interactions vs. energy for phoswich crystals (normal incidence).

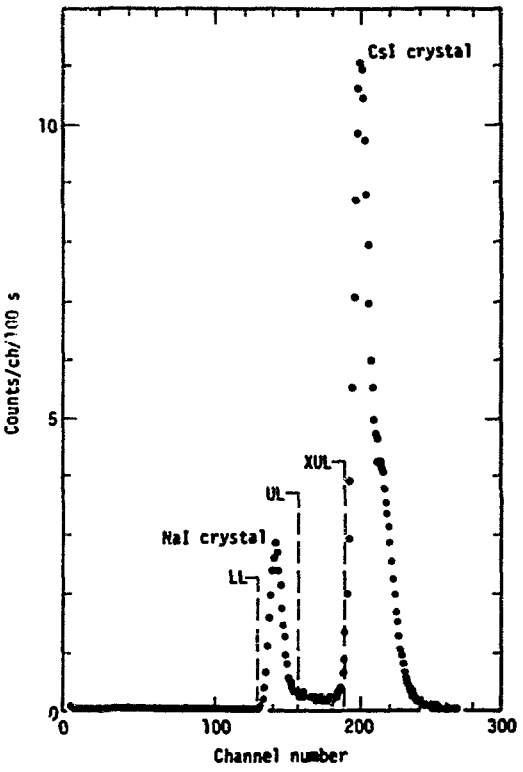

Fig. 5. Fluorescence decay time spectrum of two phoswich detectors with a ^{131}Cs source.

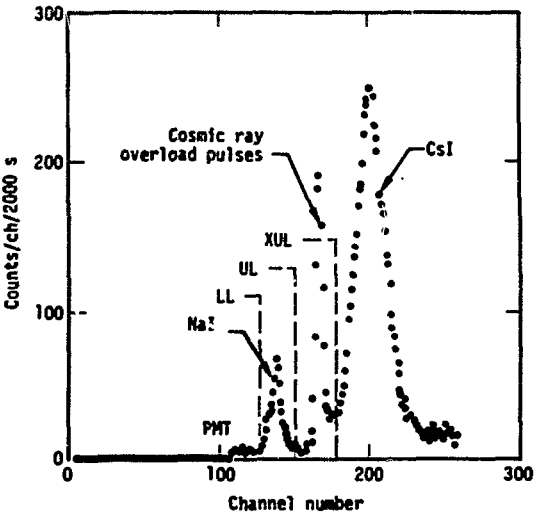

Fig. 6. Fluorescence decay time spectrum of two phoswich detectors in a shielded air background.

tillation decay time. This is accomplished by the pulse shape discrimination system shown in Fig. 1. Basically, the pulse shape analyzer (PSA) performs a time-to-amplitude conversion on the amplified detector signals, and an internal single channel analyzer (SCA) is adjusted to efficiently accept NaI events and reject all others. The lines marked LL and UL in Figs. 5 and 6 show the SCA time window selected to bracket the NaI time peak. The PSA gate output thus enables the pulse height analyzer

(PHA) only when the properly shaped signal is received. Typical low-energy spectra for ^{137}Cs and ^{241}Am obtained with this system appear in Figs. 7 and 8.

Dual Energy Analysis

The technique for extracting the higher-energy scintillation events in the CsI(Na) crystal is similar to that of the previously described NaI(Tl) crystal. That is, pulse

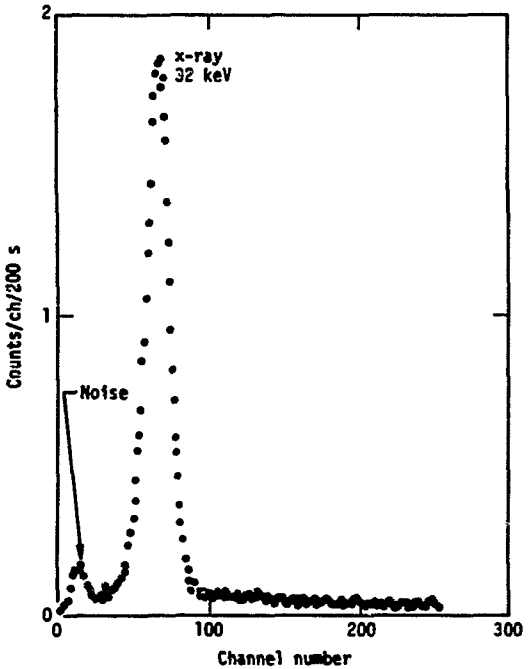

Fig. 7. Low energy ^{137}Cs spectrum with phoswich detector (calibration: 0.5 keV/ch).

shape discrimination is used to select detector signals with decay times greater than approxi- 1 μs. Figs. 5 and 6 show that no upper time limit is required, since most other signal contributors, such as PM tube noise, NaI(Tl) events, and coincident Compton-scattered events, are of shorter durations than the characteristic 1.1 μs decay time of the CsI(Na) photoelectric events. Thus, with minor modification, the same pulse shape discriminator was utilized to separately detect both NaI and CsI events, yielding an effective energy range from 5 keV to 2.5 MeV, or a 500:1 ratio.

Electronics

Figure 9 shows the block diagram of the dual energy system, which operates in the following manner. Each phoswich detector has its own high-voltage supply, which is adjusted so that both low-level detector sensitivities coincide. Each detector operates with a separate charge preamplifier whose outputs are summed into three separate amplifiers. The

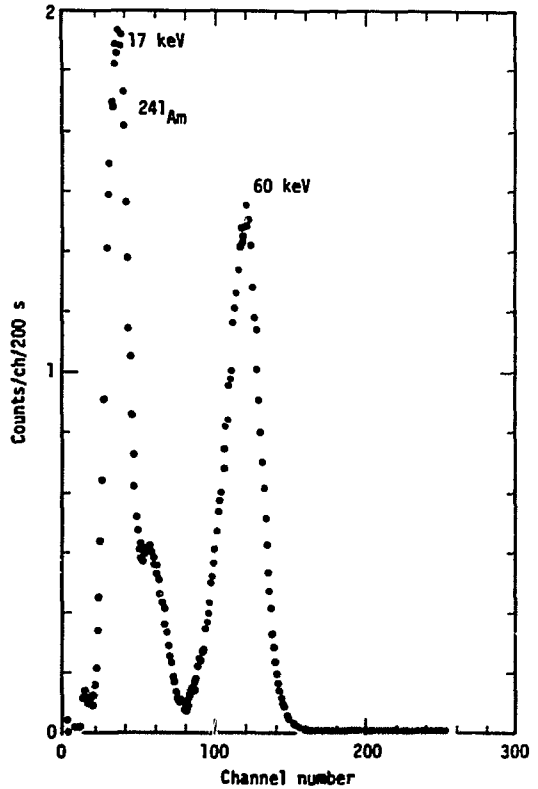

Fig. 8. Low energy ^{241}Am spectrum with phoswich detector (calibration: 0.5 keV/ch).

first amplifier is a 1 μs double delay line (DDL) type used in conjunction with the PSA. The amplifier gain is set so that the low-level NaI signals are reproduced above the amplifier noise level and the high-level CsI signals are reproduced without amplifier saturation. This requires a low-noise preamplifier and a DDL amplifier with approximately 70 dB of dynamic range, a rise time of less than 100 ns, and excellent overload recovery from cosmic ray events. The second and third 1 μs delay line (DL) shaped amplifiers are used for NaI low-level and CsI high-level pulse height analysis, respectively. High-level CsI amplifier (No. 3) has a gain trim on one of the two inputs to match the two CsI crystals and the sensitivities of the PMT's. The outputs of these two amplifiers are delayed by 3 μs and fed to separate linear gates, which pass the signals to the PHA mixer and router equipment. The linear gates are also controlled by an overload discriminator that disables the gates for 100 μs after a cosmic ray has overloaded the DDL amplifier. The PSA generates two gate signals, one for each linear gate, depending on the decay time of the detected event. The PSA accomplishes this through time discrimination of the DDL amplifier signal by using the technique of constant fraction of pulse height discrimination.[8-10]

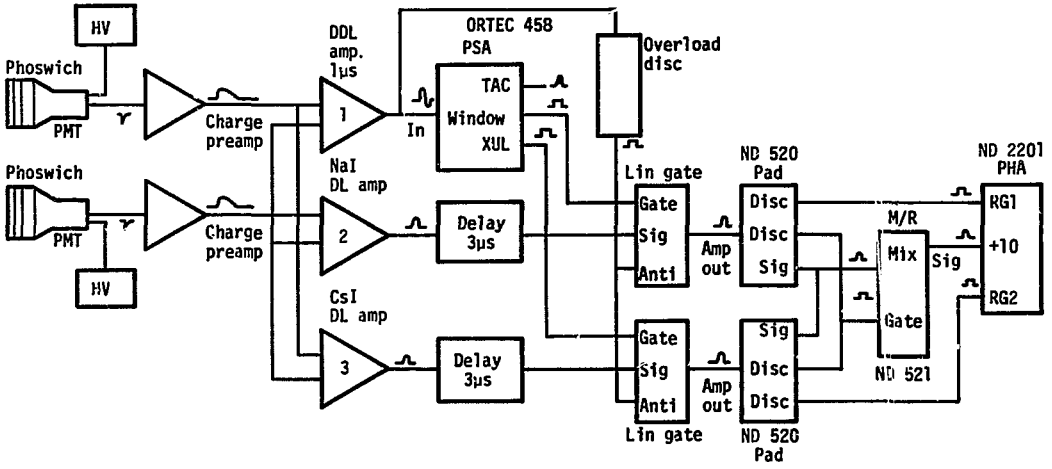

Fig. 9. Diagram of the phoswich dual energy analysis system.

The PSA is a commercial unit that has been modified by the addition of an Extra Upper Level (XUL) discriminator on its TAC output.[11] Normally, the unit produces a gate signal labeled "window" when the fall time of the input signal is within the time region bounded by the low level (LL) and upper level (UL) time controls. There is also a signal labeled UL that is generated when the fall time exceeds the window. The fall time of a DDL shaped signal is proportional to its rise time, which is proportional to the scintillation decay (see Fig. 10). Thus, the LL and UL time controls are set to bracket the NaI rise times as shown in Fig. 5. The "window" signal is used to control the low-level linear gate, allowing only the delayed NaI signals to be analyzed in quadrant 1 of the PHA. The CsI linear gate is then gated by the PSA's XUL signal, allowing the delayed CsI amplified signals to be analyzed in quadrant 2 of the PHA. Note that the XUL signal is used instead of the UL signal in order to reject Compton-scattered events. Figure 11 shows an overlay of the PSA's TAC spectrum first gated by the "window" and then gated by the XUL signals for a ^{137}Cs source with two phoswich detectors. Note the absence of the Compton-scatter rise times in Fig. 5. An air background time spectrum overlay is generated in a similar manner in Fig. 12. (The figure has been split up for clarity.) Again the coincident Compton-scattered events and cosmic ray overloads are eliminated along with PM tube noise as compared with Fig. 6.

A typical ^{137}Cs high-energy (662 keV) γ-ray energy spectrum, Fig. 13, is accumulated

Fig. 10. 1 μs DDL amplified ^{241}Am detector signal (calibration: 0.2 V/cm vertical, 0.5 μs/cm horizontal).

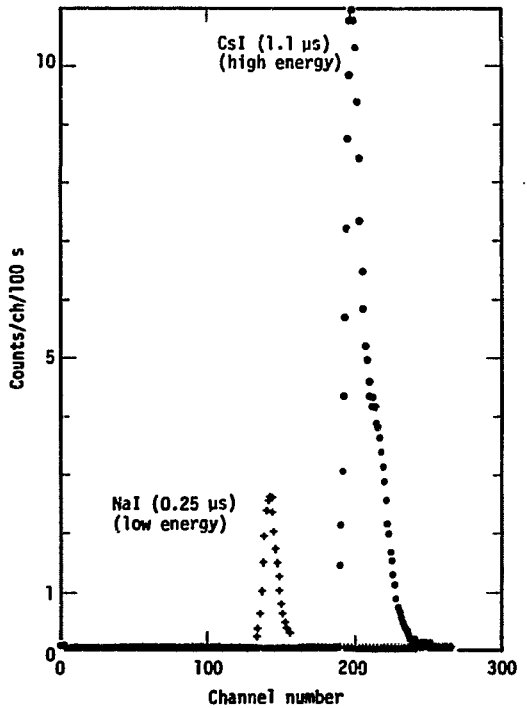

Fig. 11. PSA time spectrum gated for selection of low and high energies of ^{137}Cs from the phoswich detector.

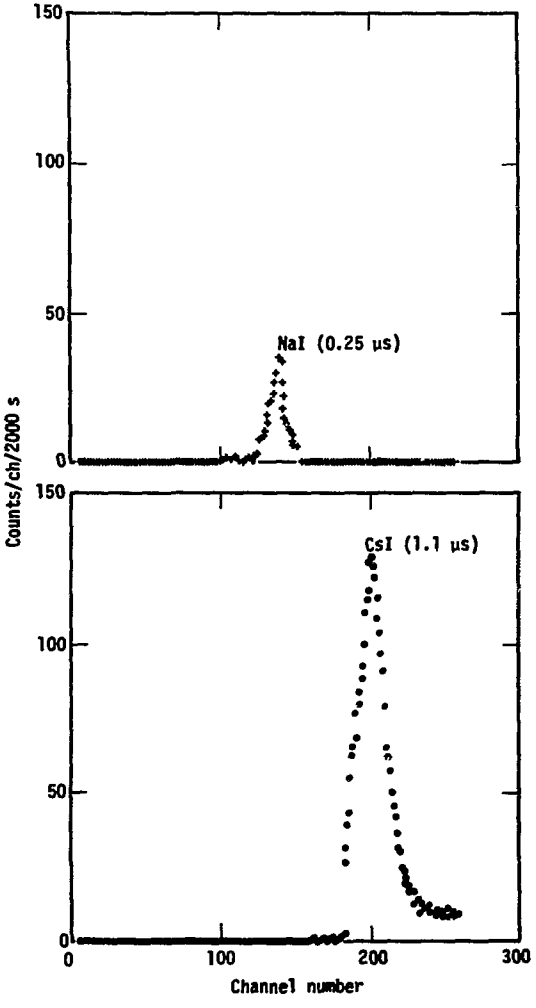

Fig. 12. PSA time spectrum of air background for the same regions selected in Fig. 11.

in the PHA's second memory quadrant. The low-energy (32 keV) x-ray spectrum of ^{137}Cs appears in the PHA's first memory quadrant and is identical to that of Fig. 7. Thus simultaneous low- and high-energy analysis is achieved at low to moderate counting rates typically encounterd with whole body or environmental sample counting.

System Performance

The following energy spectra were accumulated to display the energy analysis capabilities of the system. Figure 14 compares air background spectra that were obtained in the LLL Whole Body Counter room with a 5 in. × 1/16 in. NaI(Tl) FIDLER[12] detector, and with a 5 in. phoswich detector. This figure shows the results of the Compton suppression and

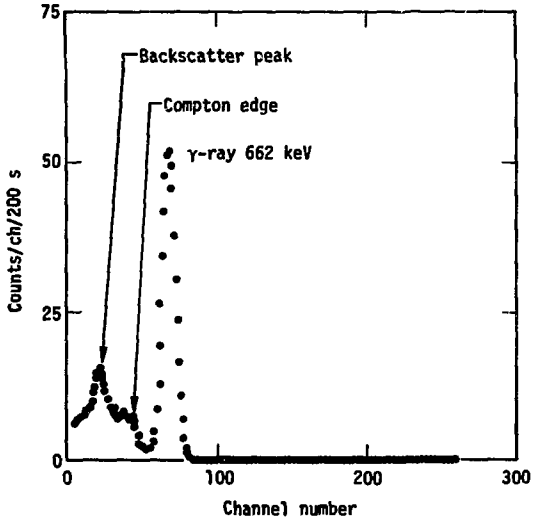

Fig. 13. High-energy ^{137}Cs spectrum with phoswich detector (calibration: 10 keV/ch).

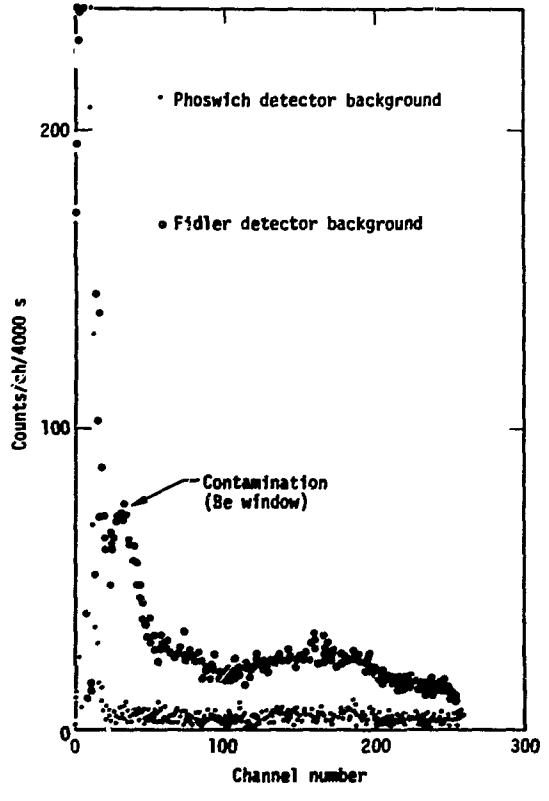

Fig. 14. Low-energy shielded air background spectra for phoswich and single-crystal FIDLER detector (calibration: 0.5 keV/ch).

noise rejection achieved with the phoswich detector system compared to a single thin crystal detector of identical size. As is apparent, there is a background reduction from 15 to 1.5 cpm (a 10:1 reduction) in the 12-24 keV region and a 15 to 1.9 cpm (7.9:1) reduction in the 50-70 keV region at 96% relative counting efficiency when using the phoswich. The reduction in the 12-24 keV region is high due to a small amount of contamination in the FIDLER Be window around 15 keV. For lower-energy x-rays such as with ^{55}Fe (5.9 keV), the phoswich counting efficiency drops to approximately 50% unless the PSA is optimized for this energy region. As noted by Landis and Goulding[13], pulse shape discrimination with a NaI detector can be utilized to eliminate low-energy PMT noise. This was investigated by using the PSA on the single-crystal detector. It yielded 50% and 38% reductions in background counts over the 12-24 keV regions, respectively, with 95% relative counting efficiency. Naturally, the contamination counts and Compton interactions were still present in the background. Thus, over the 12-24 keV and 50-70 keV regions the FIDLER-to-phoswich background ratios changed to 5.4:1 and 5.0:1, respectively, when pulse shape discrimination was used on both detectors.

Interesting results occur when both detectors, phoswich and FIDLER, are unshielded, as in the case of field operations. Figure 15 shows the unshielded background comparisons, which indicate a considerable increase in count rate. Factors of 35 and 190 for the phoswich and 16 and 73 for the FIDLER are observed over the 12-24 keV and 50-70 keV regions, respectively. The decrease in stray contamination and Compton scatter afforded by the low-background-shielded LLL Whole Body Counter[13] is very evident by this comparison since the minimum detectable activity (MDA) is proportional to the square root of the background.

Figure 16 shows the phoswich high-energy air background spectrum accumulated at the same time as Fig. 14. The natural ^{40}K peak appears along with the various Compton interactions and the positron annihilation peak. Using the XUL time discrimination instead of the UL on the CsI detector has reduced the background, mainly in the region below 1 MeV, while still maintaining 95% relative counting efficiency from 100 keV to 2.5 MeV. As seen in Fig. 4, the percentage of photoelectric, Compton, and pair production interactions for the 1 1/2-in.-thick CsI portion of the detector must be considered in determining the overall detector collection efficiency.

Subject Background

The spectra in Figs. 17(a) and 17(b) were obtained while lung counting a normal individual with no plutonium contamination. There is an appreciable increase in both the low- and high-energy spectra compared to an air background because of scattering from the body and the additional ^{40}K and ^{137}Cs present in the body.

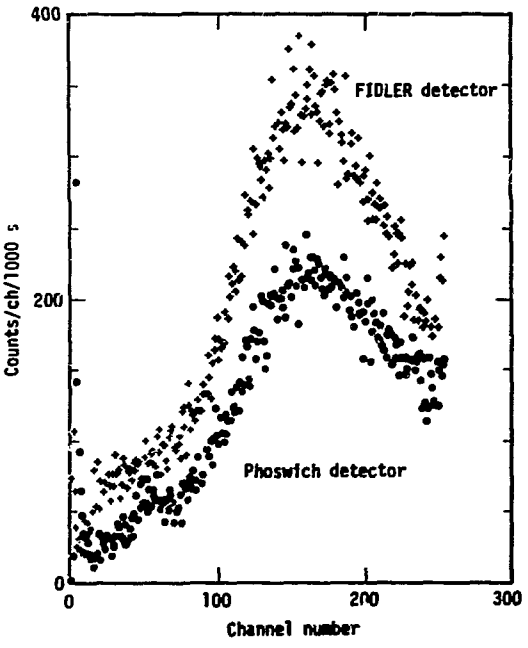

Fig. 15. Low-energy unshielded air background spectra for phoswich and single-crystal FIDLER detectors (calibration: 0.5 keV/ch).

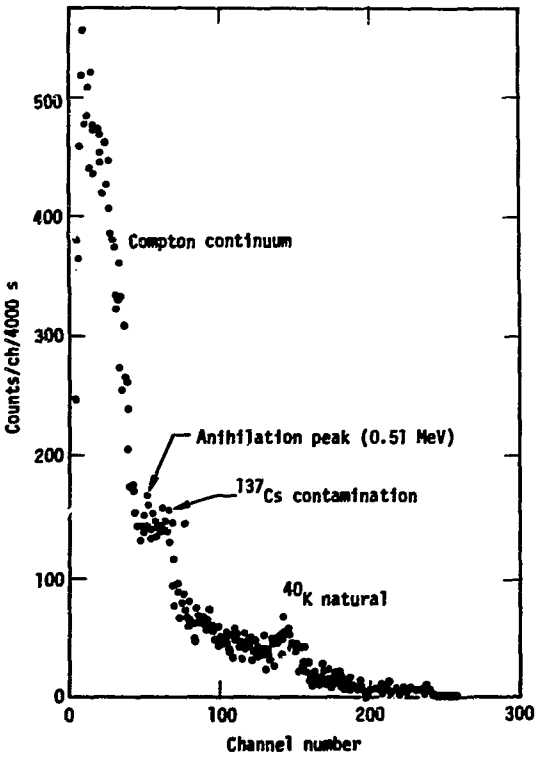

Fig. 16. High-energy shielded air background spectrum with phoswich detectors (calibration: 10 keV/ch).

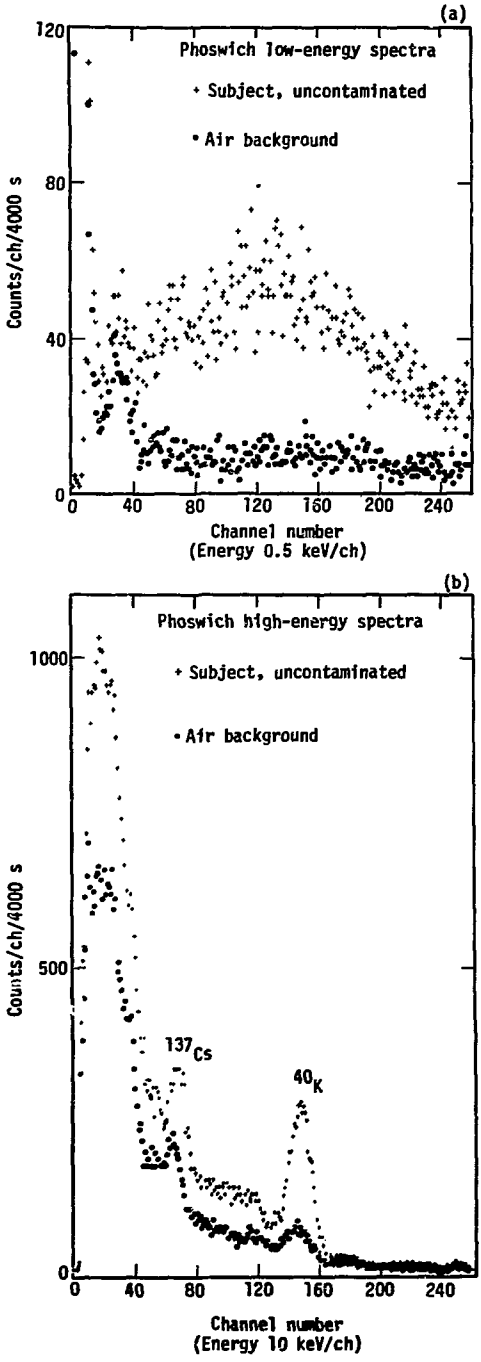

Fig. 17. (a) Normal subject low-energy lung count with phoswich detector.

(b) Normal subject high-energy spectrum from lung count in 17a.

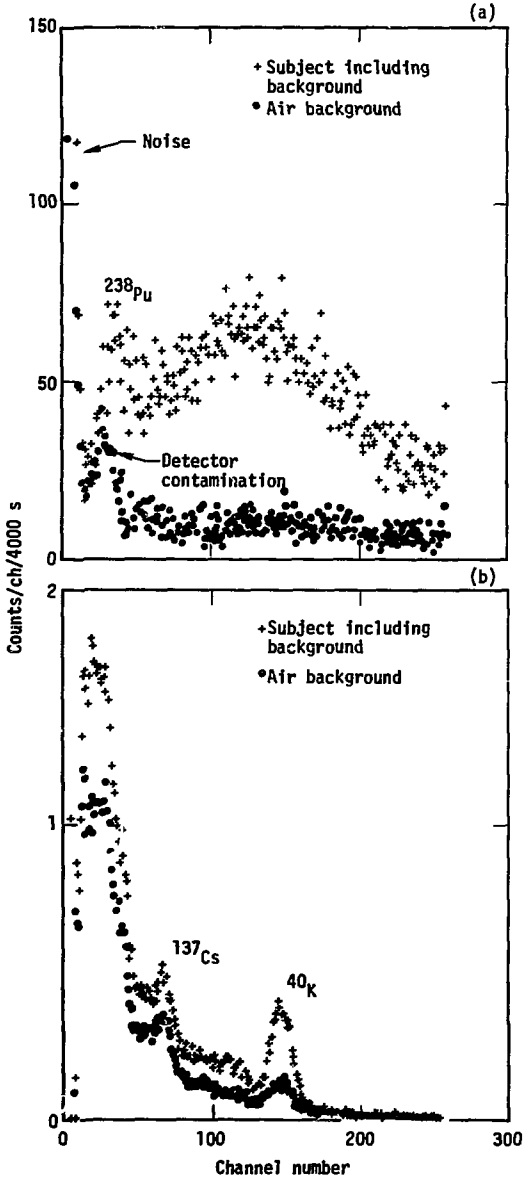

Fig. 18. (a) Contaminated subject low-energy spectrum with two phoswich detectors-33 nCi of ^{238}Pu (calibrated: 0.5 keV/ch).

(b) High-energy spectrum from lung count in 18a (calibration: 10 keV/ch).

Backgrounds in humans vary from about 3-7 cpm in the 17-keV region used for Pu analysis because of differences in the physical size and the natural radioactivity content of the individual, and these backgrounds can

easily mask the weak x-ray emission from small amounts of Pu deposited within the lung or other parts of the body. Body structures such as bone, ribs, muscle, fat, and the heart absorb the soft 17-keV x-rays, whose equivalent half-thickness in tissue is about 6 mm, to such a degree that very few x-rays are available at the body surface for counting. Detector size and counting position are also important because of variable deposition in the body.

For an average-size person with one maximum permissible lung burden of ^{239}Pu (16 nCi), only about 1-2 x-rays/min are detectable at the chest surface over the area viewed by the detectors. For this reason, it is very important to determine accurately the person's normal uncontaminated background.

The spectra in Figs. 18(a) and 18(b) were obtained from an individual with approximately 33 nCi of ^{238}Pu, or about 2 lung burdens. When these spectra are compared with one for a normal uncontaminated subject (Fig. 17(a)) of similar size, the difficulty of the assessment is apparent, even though the detector efficiency for ^{238}Pu is more than a factor of 2 greater than for ^{239}Pu. An approximate background match can often be made by carefully selecting an unexposed individual of the same height, weight, shape, and natural radioactivity content; but sometimes the right subject for comparison is not easily obtained, nor is a current, normal background usually available for the exposed subject.

It therefore becomes necessary to devise other means of assessing a person's natural, uncontaminated background. This has been done by using a portion of the x-ray spectrum at higher energy, where it is unaffected by the Pu contaminant, to predict the normal uncontaminated background in the lower-energy or Pu region of the spectrum.[14] By using the high-energy CsI spectrum from a lung count, an estimate of the scatter contribution into the low-energy spectrum can also be obtained. At present, a background study of uncontaminated laboratory personnel is being made to find the best relations of correlation between the x-ray and high energy spectra.

References

1. B.M. Shoffner, IEEE Trans. Nucl. Sci. NS19(1), 502 (1972).
2. S. Wilson, G. Baker, and K. Schlansker, IEEE Trans. Nucl. Sci. NS19(1) 512 (1972).
3. T.N. Dean, W.H. Laugham, and H.M. Ide, "External Measurement of Plutonium Lung Burdens", Los Alamos Scientific Laboratory Rept. LA-DC-10906 (1971).
4. G.R. Laurer and M. Eisenbud, in Diagnosis and Treatment of Deposited Radionuclides, H.A. Kornberg, Ed. (Excerpta Medica Foundation, N.Y., 1968).
5. C.Lam and R. Wainerdi, Trans. Amer. Nucl. Soc. 8(2), 340 (1965).
6. J.R. Watt, Savannah River Laboratory, Aiken, S.C., private communication (Nov. 1971).
7. J.H. Hubbell, Photon Cross Sections, Attenuation Coefficients, and Energy Absorption Coefficients from 10 keV to 100 GeV (U.S.G.P.O., Washington, 1969).
8. W.J. McDonald and D.A. Gedeke, Nucl. Instr. and Meth. 55, 1 (1967).
9. S. Kinbara and T. Kamahara, Nucl. Instr. and Meth. 70, 173 (1969).
10. M.R. Maier and P. Spern, Nucl. Instr. and Meth. 87, 13 (1970).
11. Ortec Instruction Manual 458 PSA, Ortec Inc., Oak Ridge, Tennessee.
12. J. Tinney and J. Koch, HC Progress Report No. 29, Lawrence Livermore Laboratory, Rept. UCRL-50007-67-3 (1967). p. 7.
13. D. Landis and F. Goulding, Nucl. Instr. and Meth. 33, 303 (1965).
14. P.N. Dean, Los Alamos Scientific Laboratory, Los Alamos, New Mexico, private communication (May 1973).